Hindawi
Journal of Analytical Methods in Chemistry
Volume 2023, Article ID 7009624, 9 pages
https://doi.org/10.1155/2023/7009624

Research Article

Highly Sensitive Immunosensing of Carcinoembryonic Antigen Based on Gold Nanoparticles Dotted PB@PANI Core-Shell Nanocubes as a Signal Probe

Dexiang Feng,[1,2] **Lingzhi Chen**,[2] **Ke Zhang**,[1,2] **Shuangshuang Zhu**,[1] **Meichen Ying**,[2] **Peng Jiang**,[2] **Menglan Fu**,[2] **Yan Wei**,[1,2] **and Lihua Li**[2]

[1]*Department of Chemistry, Wannan Medical College, Wuhu 241002, China*
[2]*Institute of Synthesis and Application of Medical Materials, Department of Pharmacy, Wannan Medical College, Wuhu 241002, China*

Correspondence should be addressed to Yan Wei; yanwei@wnmc.edu.cn and Lihua Li; llh05530226@126.com

Received 10 September 2022; Revised 1 November 2022; Accepted 23 March 2023; Published 7 April 2023

Academic Editor: Jose Vicente Ros Lis

Herein, a method was developed for the sensitive monitoring of carcinoembryonic antigen (CEA) by gold nanoparticles dotted prussian blue@polyaniline core-shell nanocubes (Au NPs/PB@PANI). First, a facile low-temperature method was used to prepare the uniform PB@PANI core-shell nanocubes with the assistance of PVP, where PB acted as the electron transfer mediator to provide electrochemical signals, and the PANI with excellent conductivity and desirable chemical stability not only played the role of a protective layer to prevent etching of PB in basic media but also effectively improved electron transfer. Importantly, to further enhance the electrical conductivity and biocompatibility of PB@PANI and to further enhance the electrochemical signal and capture a large amount of Ab_2, Au NPs were doped on the surface of PB@PANI to form Au NPs/PB@PANI nanocomposites. Subsequently, benefiting from the advantages of core-shell structure nanoprobes and gold-platinum bimetallic nanoflower (AuPt NF), a sandwich-type electrochemical immunosensor for CEA detection was constructed, which provided a wide linear detection range from 1.0 pg·mL^{-1} to 100.0 ng·mL^{-1} and a low detection limit of 0.35 pg·mL^{-1} via DPV (at 3σ). Moreover, it displayed a satisfactory result when the core-shell structure nanoprobe-based immunosensor was applied to determine CEA in real human serum samples.

1. Introduction

As we all know, carcinoembryonic antigen (CEA) is a tumor marker for colon cancer, breast cancer, ovarian cancer, and other cancers, which can provide reliable information for the early diagnosis and treatment of tumor patients [1–3]. Consequently, the highly sensitive determination of CEA is a pressing need by virtue of accurate and efficient analytical techniques. Immunosensors based on antibody-antigen interaction are one of the most widely used analytical techniques in the quantitative detection of biomarkers [4]. Among them, electrochemical immunosensors have attracted much attention due to their characteristics of high specificity, good sensitivity, short time consumption, low energy consumption and trace detection, and more suitable for the detection of biomarkers in low concentration [5, 6]. More recently, lots of electrochemical immunosensors have been constructed for quantitation of CEA. For example, Wang et al. Jozghorbani et al. and Wang et al. designed three kinds of label-free CEA immunosensors with detection limits of 0.005, 0.05, and 0.0429 ng·mL^{-1}, respectively [7–9]. Especially, a large number of reports have focused on the sandwich-type electrochemical immunosensor for CEA detection [10–13], thanks to their distinct advantages such as lower background noise, higher sensitivity, and importance, and they have higher selectivity for analytes through two specific reactions, which are superior to label-free counterparts [14–16].

Prussian blue (PB) with a face-centered cubic lattice structure is popular as a kind of electrochemical redox-active species in electrochemical biosensors because of its high electrochemical/electrocatalytic properties and low redox potential [17, 18]. Unfortunately, the poor stability and low conductivity of PB limit its further applications in biosensors [19]. To minimize these problems, some conducting materials can be introduced to meet the requirements mentioned above. Polyaniline (PANI) as one of the most desired materials with good chemical stability, low cost, and good electrical conductivity can not only provide a conductive substrate but also can form an effective coating layer on "the core" such as carbon nanotubes (CNTs) or PB [20, 21]. The combination of PB and PANI (PB@PANI) can play a significant synergistic effect and improve the electrocatalytic performance, conductivity, and stability [21]. Furthermore, to further enhance the conductivity and biocompatibility of PB@PANI, gold nanoparticles (Au NPs) were introduced over the surface of PB@PANI by Au-N bonds between Au NPs and -NH_2 from PANI to form Au NPs/PB@PANI nanocomposites [15]. To the best of our knowledge, the preparation and application of Au NPs/PB@PANI nanocomposites in electrochemical immunosensors have not been reported. Hence, the PB@PANI loaded with Au NPs (Au NPs/PB@PANI) would be a promising nanoprobe.

For sandwich-type electrochemical immunosensors, to achieve signal amplification and high sensitivity, it is a more important key to effectively immobilize the primary antibody (Ab_1) [22, 23]. Gold and platinum nanoparticles are the most promising bimetallic materials for various applications due to their superior biocompatibility, higher specific surface area, and superior electrocatalytic properties towards the reduction of H_2O_2 [24–26]. They can be decorated onto the surface of the L-cysteine (L-Cys)-modified electrode to provide an available microenvironment for loading amounts of Ab_1, thus greatly improving the sensitivity of the immunosensor.

This work was developed by electrodeposition of AuPt bimetallic nanoflower (AuPt NFs) on the GCE modified with L-Cys as a sensing platform and Au NPs/PB@PANI as a novel label prepared by a facile low-temperature method. The existence of AuPt NFs not only fixed the primary antibody but also accelerated the electron transfer. Furthermore, the as-developed Au NPs/PB@PANI nanoprobes were used as a tracer for the generation and amplification of electrochemical signals and easily captured second antibodies (Ab_2) via Au-N bond. As expected, a sandwich-type electrochemical immunosensor capable of achieving large signal amplification was developed by connecting Ab_1-AuPt NFs/L-Cys with Ab_2-Au NPs/PB@PANI.

2. Materials and Methods

2.1. Materials and Chemicals. Carcinoembryonic antigen (CEA) and its antibodies, α-fetoprotein (AFP), were purchased from Biocell Biotech. Co., Ltd. (Zhengzhou, China). Chloroauric acid ($HAuCl_4{\cdot}4H_2O$), chloroplatinic acid (H_2PtCl_6 $6H_2O$), bovine serum albumin (BSA), polyvinyl pyrrolidone (PVP), L-cysteine (L-Cys), aniline, ammonium persulfate, and so on were purchased from Aladdin Reagent Co., Ltd. (Shanghai, China).

2.2. Devices. Electrochemical measurements were made at the CHI 660E electrochemical workstation (Shanghai Co., Ltd., China). The morphology of nanomaterials was obtained by a scanning electron microscopy (SEM, JSM-7100F, Japan) and a transmission electron microscopy (TEM, JEM-6700F, Japan).

2.3. Synthesis of PB Nanocubes. PB nanocubes were synthesized according to a previous work despite a minor modification [27]. 8.0 mmoL·L^{-1} $Na_4Fe(CN)_6.8H_2O$, 4.0 mL hydrochloric acid (37%), and 2.0 g polyvinyl pyrrolidone ($M_w \sim 40000$) were added into deionized water (400 mL) and stirred for 30 min, and then were refluxed at 60°C for 6 h. After that, the blue products were washed with deionized water and dried in vacuum at 100°C for 24 h.

2.4. Preparation of PB@PANI Core-Shell Nanocubes. PB@PANI core-shell nanocubes were synthesized with reference to previous work with slight variations [21]. Briefly, 0.6 g·PB, 0.5 g polyvinyl pyrrolidone ($M_w \sim 40000$) and 100 μL aniline monomer were dissolved in 100 mL hydrochloric acid (1 moL·L^{-1}) with sonication for 1 h. Then, ammonium persulfate solution (1.6 mmoL·L^{-1}) was added dropwise into the above solution and stirred for 18 h in an ice bath. Finally, the PANI-coated PB (core-shell structure PB@PANI) was collected by centrifugation and washed with deionized water and ethanol for several times.

2.5. Preparation of Ab_2-Au NPs/PB@PANI Bioconjugates. 15 mg PB@PANI nanocubes were added into the concentrated Au NPs colloidal solution (5.0 mL, 1.0 mg·mL^{-1}) and reacted 30 min under shaking. Au NPs were assembled on the surface of PB@PANI to form the Au NPs/PB@PANI nanocomposites by the chemical bond of Au-NH_2 [15]. Followed by centrifugation and washing twice with deionized water, the obtained precipitate was redispersed into PBS solution (pH 7.0). Subsequently, 500 μL CEA-Ab_2 (2.0 mg·mL^{-1}) was added into the Au NPs/PB@PANI suspension (2 mL) and stirred for 12 h at 4°C. To get rid of nonspecific adsorption, 100 μL of 1% BSA was mixed with the obtained conjugates for 6 h at 4°C. Finally, the bioconjugates were centrifuged and redispersed in PBS (pH 7.0, 10 mmoL·L^{-1}), and then stored at 4°C.

2.6. Fabrication of the Immunosensor. For polymer nanocomposite film deposition, polished glass carbon electrode (GCE) was first immersed in 0.5 mmoL·L^{-1} cysteine containing PBS (pH 7.0) and was scanned in the potential range of −0.0 to 1.7 V at 50 mV/s for 3 cycles. The obtained electrode was dried in air, then dipped into 0.2 moL·L^{-1} H_2SO_4 and the solution containing 0.5 mmoL·L^{-1} $HAuCl_4$

and 0.5 mmoL·L^{-1} H_2PtCl_6, and electrodeposited with chronoamperometric method at −0.2 V vs. Ag/AgCl for 600 s at room temperature. After rinsing, the AuPt NFs/L-Cys/GCE-modified electrode was immersed in primary antibody (CEA-Ab_1) solution at 4°C overnight, and Ab_1 was connected to the modified electrode. Next, to remove excess binding sites, the modified electrode was immersed in 1 wt% BSA solution at room temperature for 40 min. Finally, the obtained electrode was washed three times with PBS and stored at 4°C. Scheme 1(a) displays the schematic of the designed immunosensor, and Scheme 1(b) shows the preparation procedure of Ab_2-Au NPs/PB@PANI bioconjugates.

2.7. Electrochemical Detection. The prepared immunosensors were incubated in the solutions of CEA antigen with different concentrations for 40 min and then continued incubated in Ab_2-Au NPs/PB@PANI solution at 37°C for the same time. Subsequently, differential pulse voltammetry (DPV) and electrochemical impedance spectroscopy (EIS) were performed in PBS (pH 6.5) and 5 mmoL·L^{-1} $[Fe(CN)_6]^{3-/4-}$, respectively.

3. Results and Discussion

3.1. Characterization of the Nanomaterials. SEM images of the PB, the PB@PANI, and the Au NPs/PB@PANI are displayed in Figures 1(a)–1(c). The as-prepared PB nanocomposites were made up of cubes with side lengths in the range of 300–320 nm (Figure 1(a)), which had a rough surface to provide abundant nucleation sites for the uniform growth of PANI shell [28]. It was clearly seen that the nanocubes of PB were completely covered by the PANI shell, and the thickness of the PANI was about 10 nm after the reaction time of 18 h (Figure 1(b)). When Au NPs with diameters of about 15 nm were attached to the surface of PB@PANI, we clearly observed that Au NPs with uniform globular morphology were absorbed on the surface of PB@PANI core-shell nanocubes (Figure 1(c)), which can also immobilize CEA-Ab_2 through Au-N bonds.

Figures 1(d) and 1(e) show the morphology of the electrode. As exhibited in Figure 1(d), the surface of the bare GCE was not smooth. By electrodeposition, the L-Cys film was deposited on the surface of GCE (Figure 1(e)), which maybe influence on the size and crystalline structure of AuPt bimetallic nanoflowers (AuPt NFs) according to previous reports [29]. At the same time, the presence of L-cysteine helped to bind the AuPt NFs on the surface of GCE. Quasi-spherical flower-like AuPt NFs with diameters of about 50 nm were observed after the electrodeposition on L-Cys/GCE (Figure 1(f)).

Meanwhile, Au, Pt, C, N, and S elements were found in the energy dispersive spectroscopy (EDS) of AuPt NFs/L-Cys/GCE (Figure S1A). EDS can further prove that Au NPs/PB@PANI nanocomposites were composed of Au, Pt, K, N, C, O, and Fe elements (as shown in Figure S1B).

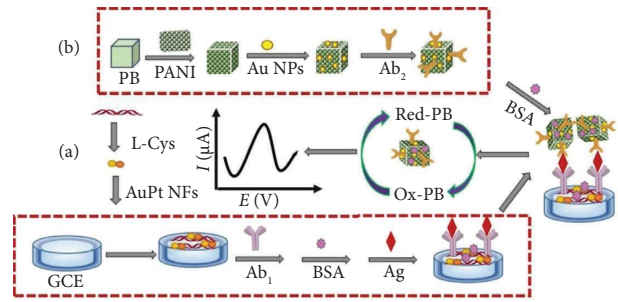

Scheme 1: (a) The construction process of electrochemical immunosensor. (b) Assembly diagram of immunoprobes.

3.2. Characterization of the Constructed Immunosensor. CV and EIS measurements were utilized to monitor the stepwise assembly process of the immunosensors [30]. As shown in Figure 2(a), the peak current of L-Cys film modified GCE electrode by one-step electropolymerization was decreased clearly (curve b) compared with the bare GCE electrode (curve a), indicating L-Cys film hindered electron transfer. In addition, modification of AuPt NFs onto the film of L-Cys caused an increase in peak current benefiting from excellent conductivity of the AuPt NFs (curve c). After Ab_1 being adsorbed on the modified electrode (curve d), blocking with BSA (curve e), and modifying with Ag (curve f), a further decrease in the peak currents was seen, due to the effect of biomacromolecules hindering electron transport. However, the peak currents increased significantly after the modified electrodes were combined with Ab_2-Au NPs/PB@PANI bioconjugates (curve g), indicating that Ab_2-Au NPs/PB@PANI bioconjugates can greatly enhance electron transfer. Moreover, EIS results of each step of electrode modification were in accordance with those of CV.

3.3. Optimization of Experimental Conditions. To improve the sensitivity and analysis efficiency of the proposed immunosensor, the experimental conditions were optimized. As shown in Figure 3(a), when incubation time was 20 min–80 min, the DPV response increased gradually and then reached a plateau after 40 min because the combination of the antigen with Ab_1 reached equilibrium in approximately 40 min.

The pH value of buffer solution has a significant influence on the stability and activity of electrochemical biosensors. As can be seen from Figure 3(b), with the change of pH, the signal of DPV response also changed. In the range of pH 5.0–8.0, DPV value first increased and then slightly decreased. Au NPs/PB@PANI nanoprobes possessed optimal activity and stability in approximately neutral or acid environment due to an effective coating layer of conducting PANI. Therefore, we chose PBS solution with a pH of 6.5 as the appropriate electrolyte.

In the meantime, the deposition time of AuPt NFs had a significant effect on DPV response as well. As displayed in Figure 3(c), as the deposition time of AuPt NFs increased

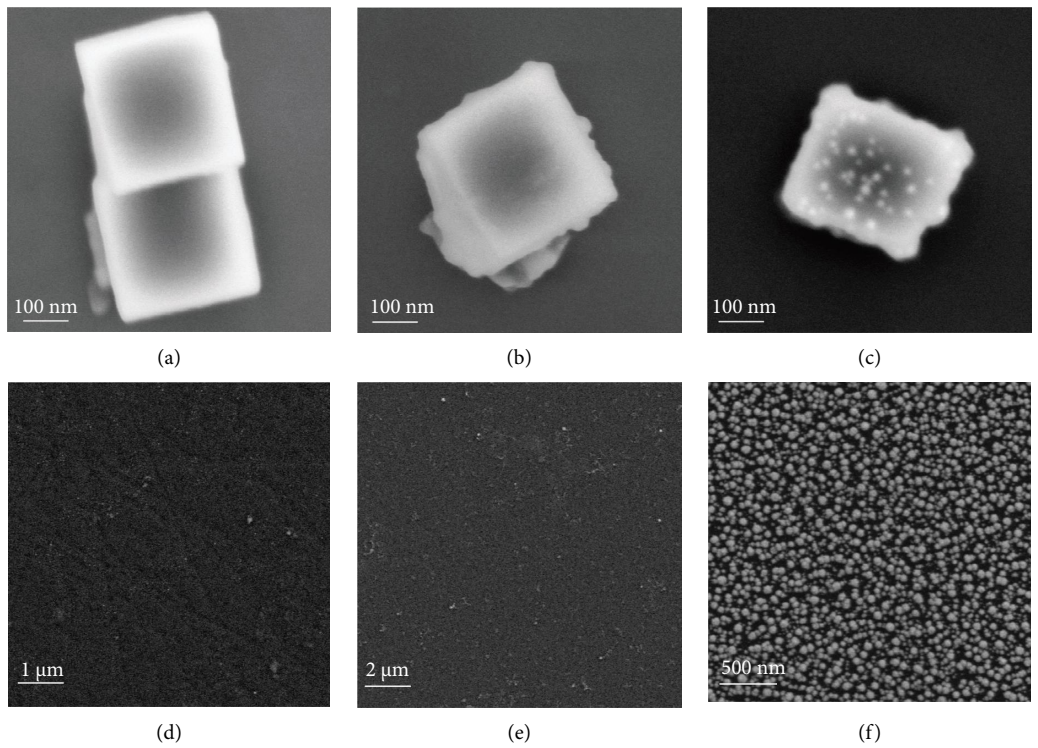

Figure 1: (a) SEM images of PB, (b) PB@PANI, (c) Au NPs-PB@PANI, (d) GCE, (e) L-Cys/GCE, and (f) AuPt NFc/L-Cys/GCE.

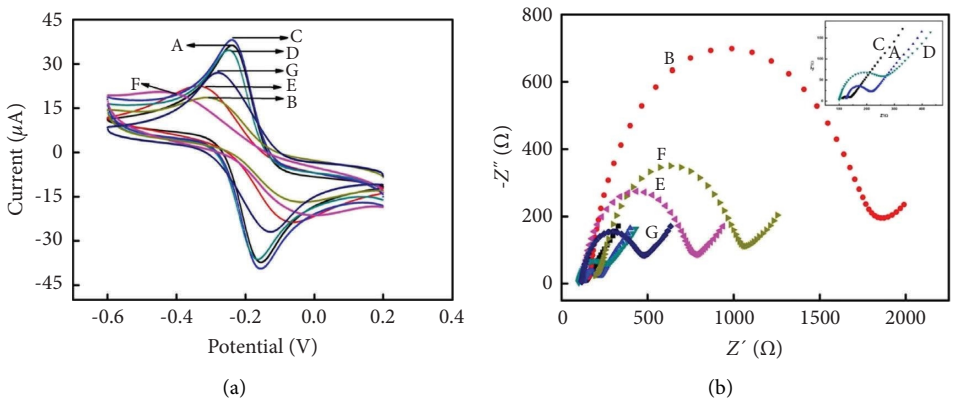

Figure 2: (a) CVs and (b) EIS of (A) bare GCE, (B) L-Cys/GCE, (C) AuPt NFs/L-Cys/GCE, (D) Ab1/AuPt NFs/L-Cys/GCE, (E) BSA/Ab1/AuPt NFs/L-Cys/GCE, (F) Ag/BSA/Ab1/AuPt NFs/L-Cys/GCE, (G) Bioconjugates/Ag/BSA/Ab1/AuPt NFs/L-Cys/GCE in $[Fe(CN)_6]^{3-/4-}$.

from 200 to 1000 s, the current signal increased gradually and then reached a plateau at 600 s. Therefore, the deposition time of AuPt NFs was selected as 600 s for the preparation of the immunosensor.

Similar to reported biosensor, the performance of immunosensor was highly affected by the concentration of Au NPs/PB@PANI. As shown in Figure 3(d), with the increasing concentration from 0.5 mg·mL^{-1} to 2.0 mg·mL^{-1}, the current response increased rapidly, but when the concentration was higher than 2.0 mg·mL^{-1}, the current response reached a plateau. Therefore, 2.0 mg·mL^{-1} became the optimum concentration for this study.

3.4. Quantitative Detection of CEA. Under optimal experimental conditions, CEA was quantified by using the developed immunosensor. As shown in Figure 4, the DPV signal increased gradually as the CEA concentration increased. There was a good linear relationship between the current intensity and the logarithm of CEA concentration in the range of 0.001–100 ng·mL^{-1}. The regression equation was $I_P(\mu A) = 4.6652 + 0.7570x$ ($R^2 = 0.9981$) with 0.35 pg·mL^{-1} detection limit. In comparison with other nanoprobe-based immunosensors [31–37], the detection limit of the prepared immunosensor was lower (Table 1). The reasons for the excellent analytical performance of the designed immunosensor

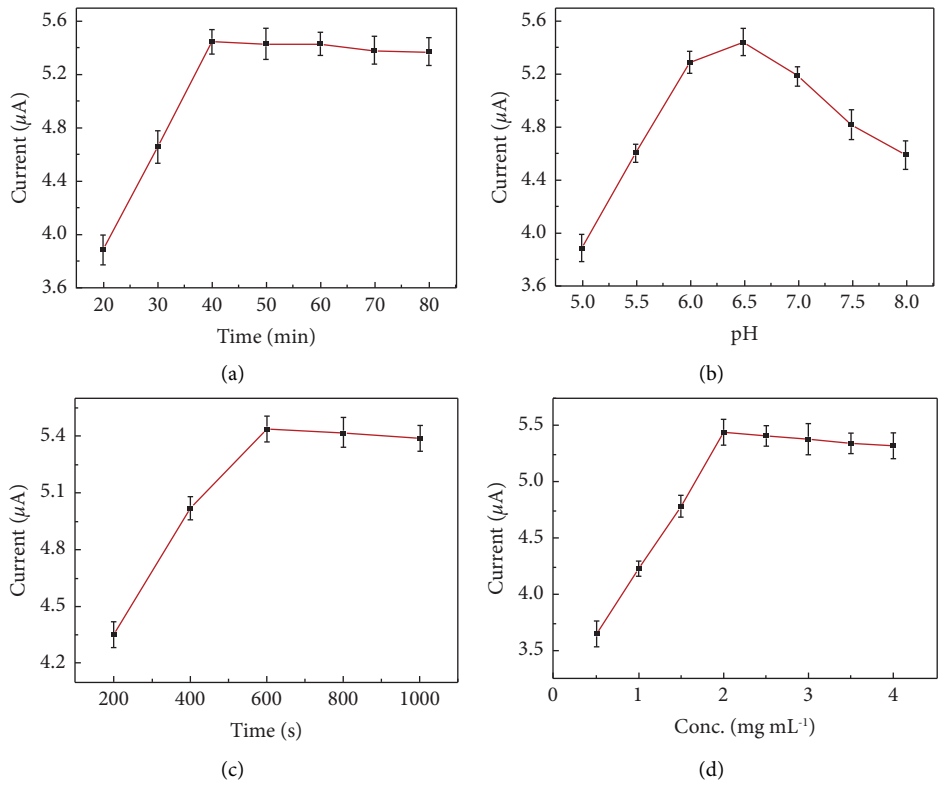

FIGURE 3: Influence of (a) incubation time, (b) pH, (c) deposition time of AuPt NFs, and (d) the concentration Au NPs/PB@PANI on the peak currents to $C_{CEA} = 10.0\,ng{\cdot}mL^{-1}$. Error bars represent standard deviations from five repeated measurements.

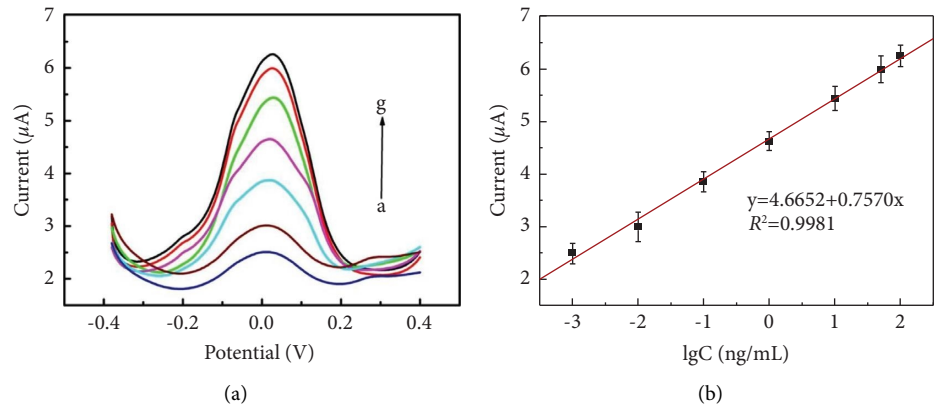

FIGURE 4: (a) DPV responses of the as-prepared immunosensor after incubation with CEA concentrations (From a–g: 0.001, 0.01, 0.1, 1.0, 10.0, 50.0, and 100 $ng{\cdot}mL^{-1}$) in 0.1 M PBS (pH 6.5). (b) Calibration curves of the immunosensor. Error bars represent standard deviations from five repeated measurements.

may be summarized as follows: first, PANI, as the conductive shell of PB@PANI core-shell structure, maintained the structural stability of PB and effectively improved the electron transfer from PANI to PB due to the intimate adhesion. Second, a large amount of Au NPs distributed on the PB@PANI surface provided a large specific surface area for the binding of antibodies, which enhanced the immobilization of CEA-Ab_2. In addition, the Au NPs/PB@PANI nanoprobes with the unique structure and synergetic contributions exhibited good conductivity and high stability, increased the conduction efficiency of signal molecules, and can be used as a signal amplification system to improve the sensitivity of detection. Finally, AuPt NFs with multifunctionality were used as an ideal sensing platform, not only can capture more Ab_1 and improve conductivity but also constituted a dual signal amplification system together with Au NPs/PB@PANI nanoprobes.

3.5. Specificity, Stability, and Reproducibility of the Immunosensor. In order to investigate the specificity of the constructed immunosensor targeting CEA, 100.0 $ng{\cdot}mL^{-1}$ of

Table 1: Comparison of analytical performance of CEA immunosensors with different nanoprobes.

Nanoprobes	Linear range ($ng{\cdot}mL^{-1}$)	Detection limit ($ng{\cdot}mL^{-1}$)	Reference
Ag-BSA-Pt NPs	0.005–100.00	7.60×10^{-4}	[31]
CPS@PANI@Au	0.006–12.00	1.56×10^{-3}	[32]
PTh-Au	0.3–30.00	1.47×10^{-4}	[33]
3D-rGO-MWCNTs/Ag-Au Ps	0.001–80.00	3.00×10^{-3}	[34]
AuNPs-PAN@CNTs	0.002–80.00	8.00×10^{-3}	[35]
CNSs@Au NPs	0.002–80.00	3.00×10^{-3}	[36]
Ce-MoF@HA/Ag-HRP	0.001–80.00	2.00×10^{-4}	[37]
AuNPs-PB@PANI	0.001–100.00	3.50×10^{-4}	This work

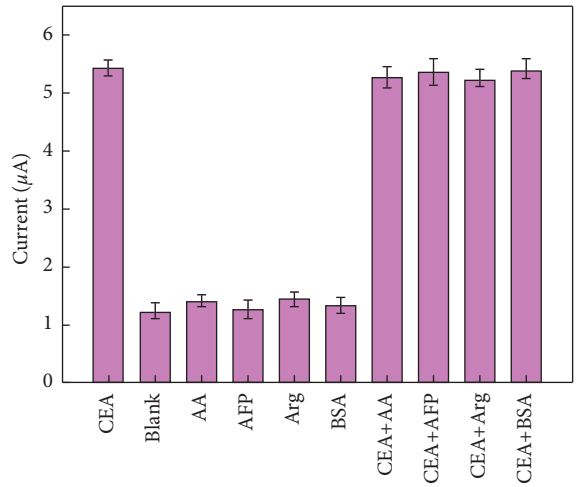

Figure 5: The specificity of the CEA immunosensor. Error bars = SD ($n = 5$).

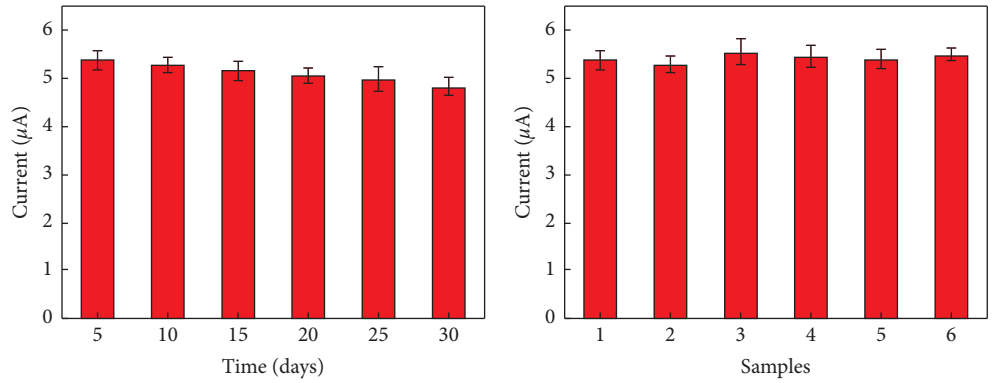

Figure 6: (a) The stability and (b) reproducibility of the CEA immunosensor. Error bars = SD ($n = 5$).

four interferences including alpha fetoprotein (AFP), ascorbic acid (AA), glucose (Glu), and BSA was added to CEA ($1.0\,ng{\cdot}mL^{-1}$) solution, respectively. As displayed in Figure 5, these interferences made a neglectful influence to the target, suggesting the proposed biosensor presented high specificity for the specific recognition of CEA.

The stability experiments of the immunosensor were carried out by storing several immunosensors at 4°C for 30 days, which were tested for CEA every 5 days (Figure 6(a)). After 30 days, the DPV value retained 88.6% of its initial response. The effective fixation of Ab_2 on the Au NPs/PB@PANI nanoprobe and the efficient protection of PB in the PANI coating made the developed immunosensor have high stability.

To further verify the reproducibility of the immunosensor, six immunosensors were incubated in $10.0\,ng{\cdot}mL^{-1}$ of CEA for DPV determination. As shown in Figure 6(b), the RSD was 3.1% after measurement, demonstrating the reproducibility of the immunosensor was acceptable.

3.6. Determination of Real Serum Sample. To certify analytical reliability and application potential of the developed immunosensor, ten clinical serum specimens containing CEA were analyzed. As displayed in Table 2, the relative

Table 2: Comparison with ELISA for CEA.

Serum sample no.	This method ($ng{\cdot}mL^{-1}$)	ELISA[a] ($ng{\cdot}mL^{-1}$)	RSD (%)
1	0.06 ± 0.01	0.058 ± 0.02	+3.45
2	0.54 ± 0.12	0.57 ± 0.08	−5.26
3	1.88 ± 0.14	1.85 ± 0.05	+1.62
4	5.00 ± 0.22	5.14 ± 0.13	−2.72
5	13.26 ± 0.42	13.76 ± 0.57	−3.63
6	18.78 ± 1.23	17.56 ± 1.65	+6.94
7	23.55 ± 1.09	24.06 ± 0.79	−2.12
8	37.67 ± 0.78	36.87 ± 1.52	+2.17
9	50.33 ± 1.77	52.26 ± 0.67	−3.69
10	78.38 ± 1.39	75.97 ± 1.83	+3.17

[a]Mean value ± SD of five measurements.

error between the two methods was in the range from −5.26% to 6.94%, and these data revealed that the developed immunosensor had good practicability for clinical serum analysis.

4. Conclusions

In conclusion, an electrochemical immunosensor based on gold nanoparticles functionalized PB@PANI core-shell nanocubes as a signal amplification strategy was fabricated for CEA detection. The high sensitivity of the immunosensor was attributed to the reasons as follows. First, the abundant N-species in PANI can be coupled with PB to effectively protect the structural degradation of PB in basic media. Second, Au NPs/PB@PANI nanocubes containing abundant electron mediators provided a large signal of DPV. Finally, AuPt NFs were dotted on the L-Cys/GCE electrode to increase the specific surface area and electrical conductivity, which not only immobilize more antibodies but also accelerate the electron transfer. Moreover, the designed immunosensor showed the especial merit that avoided the addition of mediators to the buffer or separated the immobilization of mediators onto the electrode. Promisingly, the strategy can be easily extended to the application scope of Au NPs/PB@PANI nanocomposites.

Data Availability

The data supporting this study are from previously reported studies and datasets, which have been cited.

Disclosure

A preprint of the manuscript has previously been published [38].

Conflicts of Interest

The authors declare that they have no conflicts of interest.

Acknowledgments

This work was funded from the following projects: the Anhui Provincial Natural Science Foundation (1908085MH272), the Research Fund for University Natural Science Research Project of Anhui Province (KJ2021A0842), Undergraduate Training Program on Innovation and Entrepreneurship (202010368027), the National Natural Science Foundation of China (21645006), and 2022 Anhui Provincial College Students Innovation and Entrepreneurship Training Program, College of Pharmacy 013.

Supplementary Materials

For the characterization of the signal probe material, we added the energy dispersive spectroscopy (EDS) as supplementary material, provided with the manuscript. Figure S1. EDX spectra of (A) AuPt NFs/L-Cys/GCE and (B) Au NPs/PB@PANI. (*Supplementary Materials*)

References

[1] D. L. Zheng, J. Y. Yang, Z. Y. Zheng et al., "A highly sensitive photoelectrochemical biosensor for CEA analysis based on hollow NiS@NiO/TiO_2 composite with typal p-n heterostructure," *Talanta*, vol. 246, Article ID 123523, 2022.

[2] J. Wang, J. L. Bei, X. Guo et al., "Ultrasensitive photoelectrochemical immunosensor for carcinoembryonic antigen detection based on pillar [5] arene-functionalized Au nanoparticles and hollow PANI hybrid BiOBr heterojunction," *Biosensors and Bioelectronics*, vol. 208, Article ID 114220, 2022.

[3] R. A. Miksad and N. J. Meropol, "Carcinoembryonic antigen-still more to learn from the real world," *JAMA Oncology*, vol. 4, no. 3, pp. 315-316, 2018.

[4] E. Burcu Bahadır and M. Kemal Sezgintürk, "Applications of electrochemical immunosensors for early clinical diagnostics," *Talanta*, vol. 132, pp. 162–174, 2015.

[5] S. Y. Cen, Y. G. Feng, J. H. Zhu et al., "Eco-friendly one-pot aqueous synthesis of ultra-thin AuPdCu alloyed nanowire-like networks for highly sensitive immunoassay of creatine kinase-MB," *Sensors and Actuators B: Chemical*, vol. 333, Article ID 129573, 2021.

[6] Y. Chen, X. Y. Wang, A. J. Wang et al., "Ultrasensitive ratiometric electrochemical immunoassay of *N*-terminal pro-B-type natriuretic peptide based on three-dimensional PtCoNi hollow multi-branches/ferrocene-grafted-ionic liquid and Co-N-C nanosheets," *Sensors and Actuators B: Chemical*, vol. 326, Article ID 128794, 2021.

[7] G. Y. Wang, J. Y. Chen, L. Huang, Y. T. Chen, and Y. X. Li, "A laser-induced graphene electrochemical immunosensor for label-free CEA monitoring in serum," *Analyst*, vol. 146, pp. 6631–6642, 2021.

[8] M. Jozghorbani, M. Fathi, S. H. Kazemi, and N. Alinejadian, "Determination of carcinoembryonic antigen as a tumor

marker using a novel graphene-based label-free electrochemical immunosensor," *Analytical Biochemistry*, vol. 613, Article ID 114017, 2021.

[9] Q. Wang, H. Q. Xin, and Z. Wang, "Label-free immunosensor based on polyaniline-loaded MXene and gold-decorated β-cyclodextrin for efficient detection of carcinoembryonic antigen," *Biosensors*, vol. 12, no. 8, p. 657, 2022.

[10] H. F. Shen, C. Wang, C. L. Ren et al., "A streptavidin-functionalized tin disulfide nanoflake-based ultrasensitive electrochemical immunosensor for the detection of tumor markers," *New Journal of Chemistry*, vol. 44, no. 15, pp. 6010–6014, 2020.

[11] H. Wang, J. Luo, J. G. Chen, H. Chen, T. Li, and M. H. Yang, "Electrochemical immunosensor for a protein biomarker based on the formation of prussian blue with magnetic nanoparticle," *Materials Express*, vol. 10, no. 2, pp. 278–282, 2020.

[12] X. C. Liao, C. Y. Ma, C. L. Zhao et al., "An immunosensor detects carcinoembryonic antigen by dual catalytic signal enhancer-hydrogen peroxide based on in-situ reduction of silver nanoparticles with dopamine and graphene high-load cobalt tetroxide," *Microchemical Journal*, vol. 160, Article ID 105602, 2021.

[13] J. J. Wang, X. Hua, and B. K. Jin, "Ultrasensitive detection of carcinoembryonic antigen by chitosan/polythiophene/CdTe electrochemical biosensor," *ACS Omega*, vol. 7, no. 49, pp. 45361–45370, 2022.

[14] Y. G. Feng, J. W. He, L. Y. Jiang, D. N. Chen, A. J. Wang, and J. J. Feng, "Novel sandwich-typed electrochemical immunosensing of C-reactive protein using multiply twinned AuPtRh nanobead chains and nitrogen-rich porous carbon nanospheres decorated with Au nanoparticles," *Sensors and Actuators B: Chemical*, vol. 358, Article ID 131518, 2022.

[15] F. B. Pei, P. Wang, E. H. Ma et al., "A sandwich-type amperometric immunosensor fabricated by Au@Pd NDs/Fe^{2+}-CS/PPy NTs and Au NPs/NH_2-GS to detect CEA sensitively via two detection methods," *Biosensors and Bioelectronics*, vol. 122, pp. 231–238, 2018.

[16] Y. Y. Yang, Q. Yan, Q. Liu et al., "An ultrasensitive sandwich-type electrochemical immunosensor based on the signal amplification strategy of echinoidea-shaped Au@Ag-Cu (2)O nanoparticles for prostate specific antigen detection," *Biosensors and Bioelectronics*, vol. 99, pp. 450–457, 2018.

[17] T. Li, Z. Z. Si, L. Q. Hu, H. Z. Qi, and M. H. Yang, "Prussian blue-functionalized ceria nanoparticles as label for ultrasensitive detection of tumor necrosis factor-α," *Sensors and Actuators B: Chemical*, vol. 171-172, pp. 1060–1065, 2012.

[18] S. S. Wei, H. L. Xiao, M. Gu, Z. C. Chen, and L. L. Cao, "Ultrasensitive label-free electrochemical immunosensor based on core-shell Au@PtNPs functionalized rGO-TEPA/PB nanocomposite for HBsAg detection," *Journal of Electroanalytical Chemistry*, vol. 890, pp. 115216–115224, 2021.

[19] D. X. Feng, K. Zhang, Y. Lu, J. X. Chen, and Y. Wei, "Gold microstructures/polyaniline/reduced graphene oxide/prussian blue composite as stable redox matrix for label-free electrochemical immunoassay of α-fetoprotein," *Analytical Sciences*, vol. 36, no. 12, pp. 1501–1505, 2020.

[20] Z. Kang, K. L. Jiao, J. Cheng, R. Y. Peng, S. Q. Jiao, and Z. Q. Hu, "A novel three-dimensional carbonized PANI1600@CNTs network for enhanced enzymatic biofuel cell," *Biosensors and Bioelectronics*, vol. 101, pp. 60–65, 2018.

[21] Q. Z. Zhang, L. Fu, J. Y. Luan et al., "Surface engineering induced core-shell Prussian blue@polyaniline nanocubes as a high-rate and long-life sodium-ion battery cathode," *Journal of Power Sources*, vol. 395, pp. 305–313, 2018.

[22] K. Zhang, Z. W. Cao, S. Z. Wang, J. X. Chen, Y. Wei, and D. X. Feng, "A novel sandwich-type electrochemical immunosensor based on the signal amplification strategy of core-shell Pd@Pt nanoparticles for α-fetoprotein detection," *International Journal of Electrochemical Science*, vol. 15, pp. 2604–2613, 2020.

[23] Y. Zhang, D. L. Liu, Y. Y. Zhang et al., "Highly sensitive photoelectrochemical neuron specific enolase analysis based on cerium and silver Co-Doped Sb_2WO_6," *Biosensors and Bioelectronics*, vol. 203, Article ID 114047, 2022.

[24] J. J. Feng, L. X. Chen, X. H. Ma et al., "Bimetallic AuPt alloy nanodendrites/reduced graphene oxide: one-pot ionic liquid-assisted synthesis and excellent electrocatalysis towards hydrogen evolution and methanol oxidation reactions," *International Journal of Hydrogen Energy*, vol. 42, no. 2, pp. 1120–1129, 2017.

[25] Z. G. Liu, H. D. Forsyth, N. Khaper, and A. C. Chen, "Sensitive electrochemical detection of nitric oxide based on AuPt and reduced graphene oxide nanocomposites," *Analyst*, vol. 141, no. 13, pp. 4074–4083, 2016.

[26] X. Cao, N. Wang, S. Jia, L. Guo, and K. Li, "Bimetallic AuPt nanochains: synthesis and their application in electrochemical immunosensor for the detection of carcinoembryonic antigen," *Biosensors and Bioelectronics*, vol. 39, no. 1, pp. 226–230, 2013.

[27] Y. You, X. L. Wu, Y. X. Yin, and Y. G. Guo, "High-quality prussian blue crystals as superior cathode materials for room-temperature sodium-ion batteries," *Energy & Environmental Science*, vol. 7, no. 5, pp. 1643–1647, 2014.

[28] B. Kong, C. Selomulya, G. F. Zheng, and D. Y. Zhao, "New faces of porous prussian blue: interfacial assembly of integrated heterostructures for sensing applications," *Chemical Society Reviews*, vol. 44, no. 22, pp. 7997–8018, 2015.

[29] X. X. Weng, Y. Liu, Y. Xue, A. J. Wang, L. Wu, and J. J. Feng, "L-Proline bio-inspired synthesis of AuPt nanocalliandras as sensing platform for label-free electrochemical immunoassay of carbohydrate antigen 19-9," *Sensors and Actuators B: Chemical*, vol. 250, pp. 61–68, 2017.

[30] C. C. Li, Y. X. Li, Y. Zhang et al., "Signal-enhanced electrochemiluminescence strategy using iron-based metal-organic frameworks modified with carboxylated Ru (II) complexes for neuron-specific enolase detection," *Biosensors and Bioelectronics*, vol. 215, Article ID 114605, 2022.

[31] W. T. Zhao, M. Wu, L. S. Mei, and H. L. Li, "Ultra-sensitive electrochemical determination of carcinoembryonic antigen by a sandwich immunosensor graphene oxide (GO)-Gold substrate and a silver-coated bovine serum albumin (BSA)-platinum nanocomposite on a glassy carbon electrode (GCE)," *Analytical Letters*, vol. 55, no. 6, pp. 980–989, 2022.

[32] D. D. Song, J. Zheng, N. V. Myung, J. L. Xu, and M. Zhang, "Sandwich-type electrochemical immunosensor for CEA detection using magnetic hollow Ni/C@SiO_2 nanomatrix and boronic acid functionalized CPS@PANI@Au probe," *Talanta*, vol. 225, Article ID 122006, 2021.

[33] Y. X. Lai, H. Huang, Z. H. Xia, S. Li, Y. Deng, and X. Y. Liu, "A sandwich-type electrochemical immunosensor using polythionine/AuNPs nanocomposites as label for ultrasensitive detection of carcinoembryonic antigen," *Materials Express*, vol. 9, no. 5, pp. 444–450, 2019.

[34] Y. X. Yang, K. H. Cao, M. Wu, C. L. Zhao, H. L. Li, and C. L. Hong, "3D graphene/MWNTs nano-frameworks embedded Ag-Au bimetallic NPs for carcinoembryonic antigen

detection," *Microchemical Journal*, vol. 148, pp. 548–554, 2019.

[35] D. X. Feng, L. H. Li, X. Fang, X. W. Han, and Y. Z. Zhang, "Dual signal amplification of horseradish peroxidase functionalized nanocomposite as trace label for the electrochemical detection of carcinoembryonic antigen," *Electrochimica Acta*, vol. 127, pp. 334–341, 2014.

[36] L. H. Li, Y. Wei, S. P. Zhang, X. S. Chen, T. L. Shao, and D. X. Feng, "Electrochemical immunosensor based on metal ions functionalized CNSs@Au NPs nanocomposites as signal amplifier for simultaneous detection of triple tumor markers," *Journal of Electroanalytical Chemistry*, vol. 880, pp. 114882–114887, 2021.

[37] W. J. Li, C. Y. Ma, Y. J. Song, C. L. Hong, X. W. Qiao, and B. C. Yin, "Sensitive detection of carcinoembryonic antigen (CEA) by a sandwich-type electrochemical immunosensor using MOF-Ce@HA/Ag-HRP-Ab_2 as a nanoprobe," *Nanotechnology*, vol. 31, no. 18, Article ID 185605, 2020.

[38] D. X. Feng, L. Z. Chen, M. Fu et al., "Highly sensitive immunosensing of carcinoembryonic antigen based on gold nanoparticles functionalized PB@PANI core-shell nanocubes as a novel signal amplification strategy," *SSRN Electronic Journal*, 2021.